[Frontiers in Bioscience, Landmark, 25, 463-479, Jan 1, 2020]

Hyperoside exerts potent anticancer activity in skin cancer

Yinghui Kong[1], Weiguo Sun[1], Pengfei Wu[2]

[1]Department of Dermatology, The Affiliated Huaian No. 1 People's Hospital of Nanjing Medical University, Huai'an, Jiangsu 223300 P.R. China, [2]Department of Orthopaedics, The Affiliated Huaian No. 1 People's Hospital of Nanjing Medical University, Huai'an, Jiangsu 223300 P.R. China

TABLE OF CONTENTS

1. ABSTRACT

Quercetin-3-O-β-D-galactopyranoside, is a hyperoside flavonol glycoside with anti-cancer, anti-inflammatory, and anti-oxidant activities that is derived from Hypericum and Crataegus plants. To this end, we examined the effect of this hyperoside in skin cancer cells lines and in DMBA/TPA induced skin tumors *in vivo*. *In vitro* treatment of cancer cells with hyperoside significantly inhibited phosphoinositide 3-kinase (PI3K)/protein kinase B (Akt)/mammalian target of rapamycin (mTOR)/p38 MAPK axis, concomitantly activated the 5'AMP-activated protein kinase (AMPK) signaling, inhibited proliferation, and induced apoptosis and autophagy. Hyperoside markedly inhibited diffuse epidermal hyperplasia and significantly reduced the changes in phosphorylated levels of PI3K, AKT, mTOR and AMPK while reducing p38 phosphorylation as well as of tumor burden *in vivo* in DMBA/TPA induced skin tumors. These data suggest that hyperoside might be of therapeutic value in chemoprevention of skin cancer.

2. INTRODUCTION

Nonmelanoma skin cancers (NMSC) include squamous cell carcinoma (SCC) and basal cell carcinoma (BCC) that account, respectively, for about 20% and 80% of all diagnosed NMSC cases in the world (1-2). However, some report a higher prevalence for SCC as compared to BCC (3). Apart

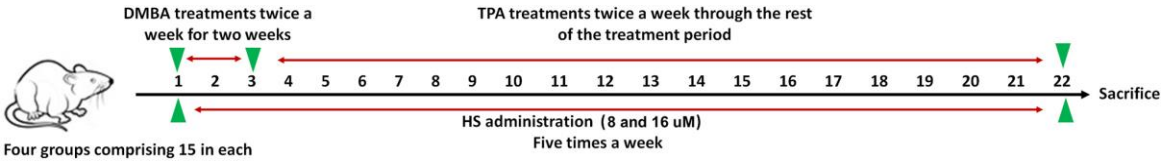

Figure 1. The procedures for animal experiments as described in the materials and methods.

from ultraviolet radiation (UVR), the common factors causing NMSC are occupational and environmental exposures to polycyclic aromatic hydrocarbons (PAHs), arsenic, as well as the ionizing radiation (4). PAHs, which are known for their toxic, carcinogenic and mutagenic effects, are produced during the incomplete combustion of organic materials, like petroleum, wood and coal (5). Among the PAHs, 7, 12 dimethylbenz(a)anthracene (DMBA) and 12-O-tetradecanoylphorbol-13-acetate (TPA) are commonly used as a model for studying carcinogenesis of SCC, a multistep process that goes through initiation, promotion and formation of cancer (6-8). Impeding or reversal of such a process can be achieved by chemoprevention (9). One category of drugs considered for such chemoprevention is flavonoids, polyphenol compounds such as hyperoside (HS), that are derived from various plants (10-14) (Figure 1). SCCs undergo both apoptosis or programmed cell death (PCD) and autophagy (15). Thus, it follows that enhancement of these processes might stop or reverse the carcinogenesis. To this end, here, we examined the effect of hyperoside on cell proliferation, apoptosis and autophagy *in vitro* in a series of SCC cell lines and *in vivo* in SCCs that were induced by topical application of DMBA/TPA to skin.

3. MATERIALS AND METHODS

3.1. Cells and treatments

Squamous cell carcinoma cell lines (A431, A432, HS-4) were obtained from American Type Culture Collection (Manassas, VA). Normal human skin cells (HACAT, HFF) were obtained from KeyGENE Biotech (Nanjing, China). Cell lines were cultured and maintained at 37 °C in MEM containing 10% FBS (GIBCO, USA) and 1% penicillin/streptomycin (GIBCO, USA) in a humidified atmosphere in presence of 5% CO_2. Hyperoside (>98% purity) was purchased from Wako-Chem (Osaka, Japan), dissolved in DMSO and stored at –20°C until further use. Upon thawing, hyperoside was diluted in DMEM medium at the indicated concentrations, with a final concentration of no more than 0.1% (v/v) DMSO.

3.2. Animals and treatments

All experimental procedures were approved by the Research Ethical Committee of Huai'an First People's Hospital, Nanjing Medical University. All experiments were performed following the Guide for the Care and Use of Laboratory Animals. A total of 60, 6–7 week-old female mice were obtained from Institute of Cancer Research (Shanghai, China). Animals were kept, in germ-free conditions, in climate-controlled quarters with a 12 h light and dark cycle, and were fed *ad libitum* with food and water. Fifteen mice were randomly assigned into four groups as follows

1. Group I: This group that serves as negative control received only the solvent vehicle (DMSO).
2. Group II: This group was treated with indicated doses of DMBA/TPA (Sigma Aldrich, USA).
3. Group III: This group was treated with indicated dose of DMBA/TPA and 8 μM HS.
4. Group IV: This group was treated with indicated dose of DMBA/TPA and 16 μM HS.

SCCs were induced by intra-dermal injection of 60 μg of DMBA in skin of the back of the animals. Two weeks later, the animals received intra-dermal injection of 4 μg TPA twice a week for a total of 22 weeks. The effect of hyperoside was examined by 1 min topical skin application of either 8 or 16 μM HS dissolved in DMSO/acetone 1:9 (V/V), 30 min before DMBA/TPA mixture was introduced to skin. The control animals received the vehicle alone. The

injections were carried out five days a week for 22 weeks, after which the size of tumors were measured with a caliper and the animals were sacrificed, the normal skin and tumors were removed and were immediately stored in liquid nitrogen, or fixed 10% Formalin.

3.3. Cell viability analysis

1×10^3 cells/well were seeded in 96-well plates (Corning, USA) containing complete growth medium. On the following day, all cells were treated with different concentrations of hyperoside (0, 1, 5, 10, 25, 50 and 100 µM) and incubated at 37 °C for 0, 12, 24 and 48 h. Then, the cell viability was measured using 3-(4,5-dimethylthiazol-2-yl)-2,5-diphenyl-2H-tetrazolium bromide (MTT) Cell Viability Assay Kit (Abnova, USA). Briefly, post hyperoside treatment, 15 µL of MTT reagent was added to each well and incubated for 4 hours at 37°C. Later, 100 µL of the solubilizer was added to each well and mixed gently on an orbital shaker for 1 hour at room temperature. Then, optical density was measured at 570 nm on an absorbance plate reader (Elx800TM absorbance microplate reader, BioTek Instrument, Inc., Vermont). Each experiment was repeated three times.

3.4. Flow cytometric assay

Apoptosis was analyzed by the Annexin V-FITC/ propidium iodide (PI) apoptosis detection kit from KeyGENE (Nanjing, China). Cells were harvested and washed with cold PBS twice and processed according to manufacturer's instructions. In brief, cells were treated with 100 µl binding buffer containing annexin V-FITC and PI and incubated on ice for 15 min in the dark. Then, 400 µL ice-cold binding buffer was added to cells and these were analyzed by a flow cytometer (BD Biosciences, USA) (16).

3.5. Migration analysis

1×10^5 skin cancer cells/well were seeded in the top chamber of 24-well Transwell micropore polycarbonate membrane filter, with a pore size of 8-µm (Millipore, USA).After 24 h, cells on the top surface of membrane were gently removed, and cells that migrated onto the bottom surface of wells stained and then counted in five random fields, under a light microscope.

3.6. Scratch wound-healing assay

Human skin cancer cells were seeded in a 6-well plate and once reaching confluence, a thin "wound" was introduced by scratching the monolayer with a pipette tip. Cells then were washed with PBS and images were captured under an inverted scope along the length of the scratch at 0 h and 24 h after introduction of the wound.

3.7. Western blot analysis

Western blot analysis was performed as previously described (17). Briefly, cells were rinsed with ice-cold PBS three times and lysed in ice-cold lysis buffer in the presence of a freshly prepared protease inhibitor cocktail. For carrying Western blotting on skin and skin tumors, 100 mg of frozen tissue were also lysed in 1ml lysis buffer (pH 7.4, 50 mM Tris-HCl, 150 mM NaCl, 1 mM NaF, 1 mM ethyleneglycol-bis(aminoethylether)-tetraacetic acid, 1% NP-40, 1 mM phenylmethane-sulfonyl fluoride, and 10 µg/ml leupeptin). Following centrifugation of the lysates at x12,000 g for 20 min at 4°C, the total protein concentration in the lysates were quantified by BSA protein assay kit (Thermo, USA). Then, 40 ng of protein extracts were resolved in 10%-12% SDS-PAGE, and then blotted to polyvinylidene fluoride membrane (PVDF) (Millipore, USA). The membranes were blocked for 2 hr with 5% skim fat dry milk dissolved in 0.1% Tween-20 and Tris-Buffered Saline (TBS). Membranes were incubated, overnight at 4°C, with primary antibodies (Table 1) dissolved in blocking buffer. Bands were revealed by chemiluminescence using Pierce ECL Western Blotting Substrate reagents (Thermo Scientific). All experiments were performed in triplicates and validated three times.

3.8. Hematoxylin and eosin staining

Formalin fixed skin and tumor tissues of experimental mice were embedded in paraffin blocks and sectioned at 3 µm thickness. Sections

Table 1. Primary antibodies used in Western blot analysis

Primary antibodies	Dilution ratio	Corporation
Rabbit anti-p-AURKA	1:1000	Abcam
Rabbit anti-AURKA	1:1000	Abcam
Rabbit anti-Bcl-2	1:1000	Cell Signaling Technology
Rabbit anti-Bcl-xl	1:1000	Cell Signaling Technology
Rabbit anti-Caspase-3	1:1000	Abcam
Mouse anti- Caspase-9	1:1000	Abcam
Rabbit anti-PARP	1:1000	Cell Signaling Technology
Rabbit anti-Cyto-c	1:1000	Abcam
Rabbit anti-Apaf-1	1:1000	Abcam
Rabbit anti-PTEN	1:1000	Abcam
Rabbit anti-Beclin-1	1:1000	Cell Signaling Technology
Rabbit anti-LC3-I/II	1:1000	Cell Signaling Technology
Rabbit anti-p-PI3K	1:1000	Cell Signaling Technology
Rabbit anti-PI3K	1:1000	Cell Signaling Technology
Rabbit anti-AKT	1:500	Cell Signaling Technology
Rabbit anti-p-AKT	1:1000	Cell Signaling Technology
Rabbit anti-p-mTOR	1:1000	Abcam
Rabbit anti- mTOR	1:1000	Abcam
Rabbit anti-p-AMPK	1:1000	Abcam
Rabbit anti-AMPK	1:1000	Abcam
Rabbit anti- p38	1:1000	Cell Signaling Technology
Rabbit anti-p-p38	1:1000	Cell Signaling Technology
GAPDH	1:200	Santa cruz

were de-paraffinized, rehydrated in descending series of alcohol and stained with hematoxylin and eosin (H&E) stain. The thickness of epidermis was measured by using Magnuspro software and in H&E staining sections by Image-J software (USA).

3.9. Immunohistochemical staining

The tissue sections were subjected to a pH based antigen retrieval, by exposing the sections to HCl (3.5 M) for 20 min at room temperature. Sections were then washed in PBS for 3 times. Following quenching of endogenous peroxidase by immersion of sections in peroxidase (0.3%), the tissue sections were incubated with normal goat serum (5%) for 30 min followed by incubation with the anti-Ki67 primary antibody (1:100 dilution; ab15580, Abcam, USA) for 2 h at room temperature. The sections were then incubated with HRP-conjugated secondary antibody, and after the sections were washed in PBS, they were developed using diaminobenzidine (DAB, ChemService, USA).

3.10. Statistical analysis

Data were expressed as the means ± standard errors of the mean (S.E.M.). Statistical analysis was carried out using GraphPad PRISM (version 6.0; Graph Pad Software) and ANOVA with Dunnet's least significant difference. A p-value of less than 0.05 was considered to be statistically significant.

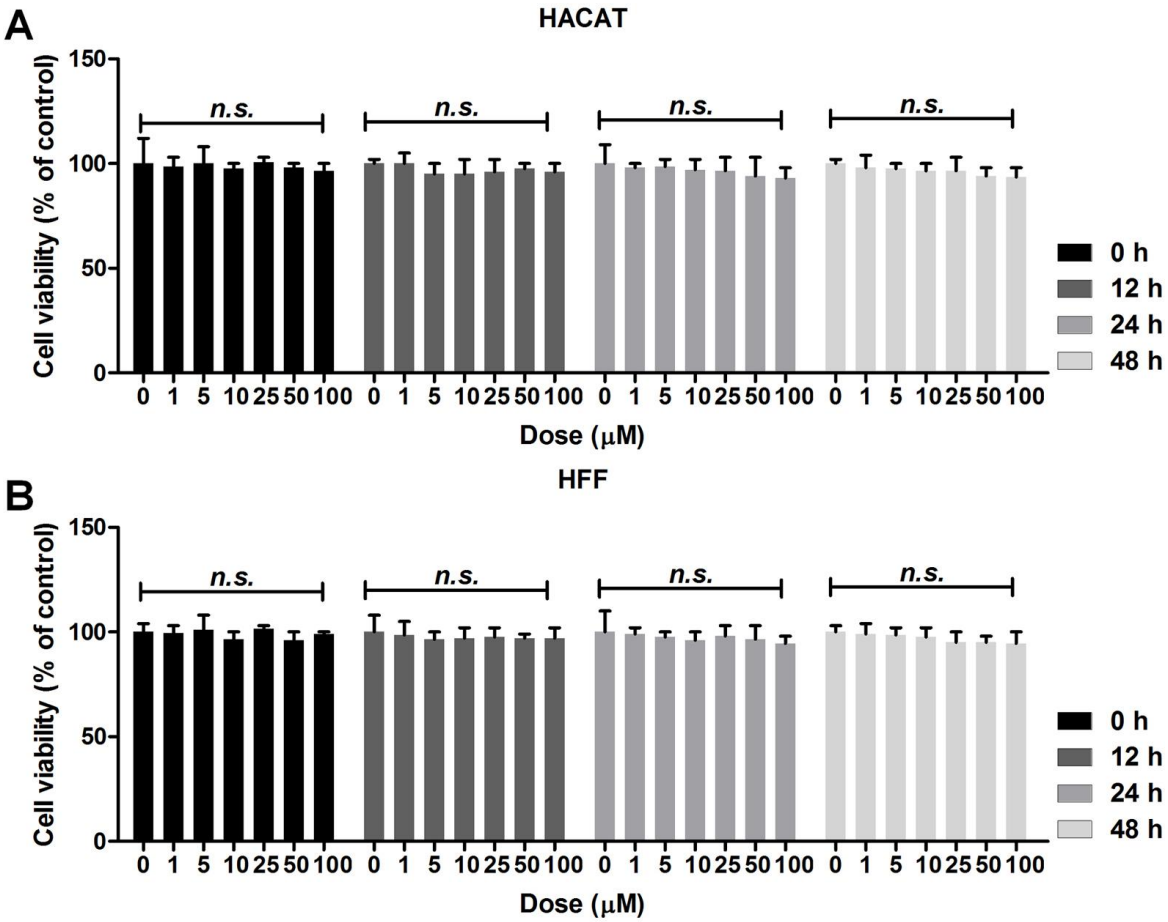

Figure 2. Hyperoside exerts no toxicity to normal skin cells, *in vitro*. Human normal skin cells (A) HACAT and (B) HFF were exposed to the indicated concentrations of hyperoside for 0, 12, 24 and 48 h. Next, MTT analysis was used to evaluate cell viability. Results are shown as mean ± SEM (n = 8 in each group). $^{*}p < 0.05$, $^{**}p < 0.01$ and $^{***}p < 0.001$ versus the Control group without any treatment.

4. RESULTS

4.1. Hyperoside reduces viability, migration, colony formation, apoptosis and autophagy of skin cancer cells *in vitro*

Hyperoside treatment did not impact the viability of HACAT and HFF normal human skin cell lines (Figure 2 A-B) whereas the viability was significantly reduced in A431, A432 and HS-4 cancer ce lls that were treated for 0, 12, 24 and 48 h with escalating doses of hyperoside (0, 1, 5, 10, 25, 50 and 100 μM) (Figure 3 A-D). This treatment increased apoptosis and reduced the migration, and colony formation in cancer cells (Figure 4-5). Moreover, consistent with such results, there was down-regulation of Bcl-2 and Bcl-xl that protect cells from apoptosis whereas the pro-apoptotic signals, Bax and Bad were upregulated (Figure 6). In addition, there was an increase in the executors of apoptosis including cytochrome C, caspase-9, caspase-3 as well as evidence for PARP cleavage (Figure 6). Examining the PTEN, Beclin-1 and LC3I/II that participate in the autophagic cell death showed that these were all increased in cells that were treated with hyperoside in a dose dependent manner while those that inhibit autophagic cell death, namely, phosphorylated levels of PI3K/AKT/mTOR were reduced (20-21, 27)(Figure 7 A-B). The phosphorylated AMPK and MAPK that maintain

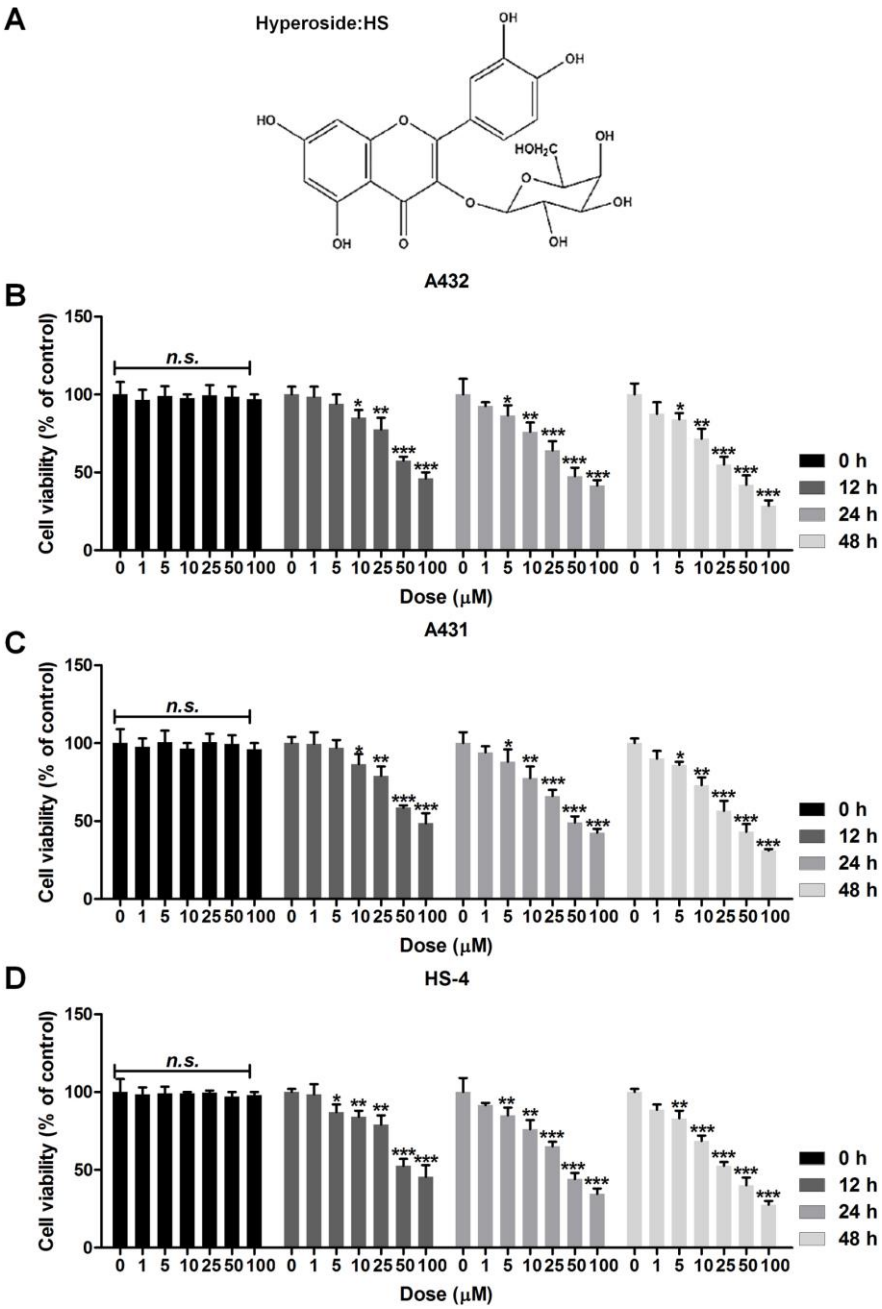

Figure 3. Hyperoside inhibits proliferation of skin cancer cells. (A) The chemical structure of hyperoside. Human skin cell lines, including (B) A432, (C) A431, and (D) HS-4, were treated with the indicated concentrations of hyperoside, ranging from 0 to 100 μM for 0, 12, 24 and 48 h. Then, the cells were harvested for MTT analysis to evaluate cell viability. Results are shown as mean ± SEM (n = 8 in each group). $^{*}p < 0.05$, $^{**}p < 0.01$ and $^{***}p < 0.001$ versus the control group without any treatment.

energy homeostasis and survival were increased in cancer cells treated with hyperoside (Figure 7 C). Consistent with reduced proliferation, phosphorylated AURKA that is increased in cells undergoing mitosis (18), was reduced in skin cancer cells treated with hyperoside (Figure 8).

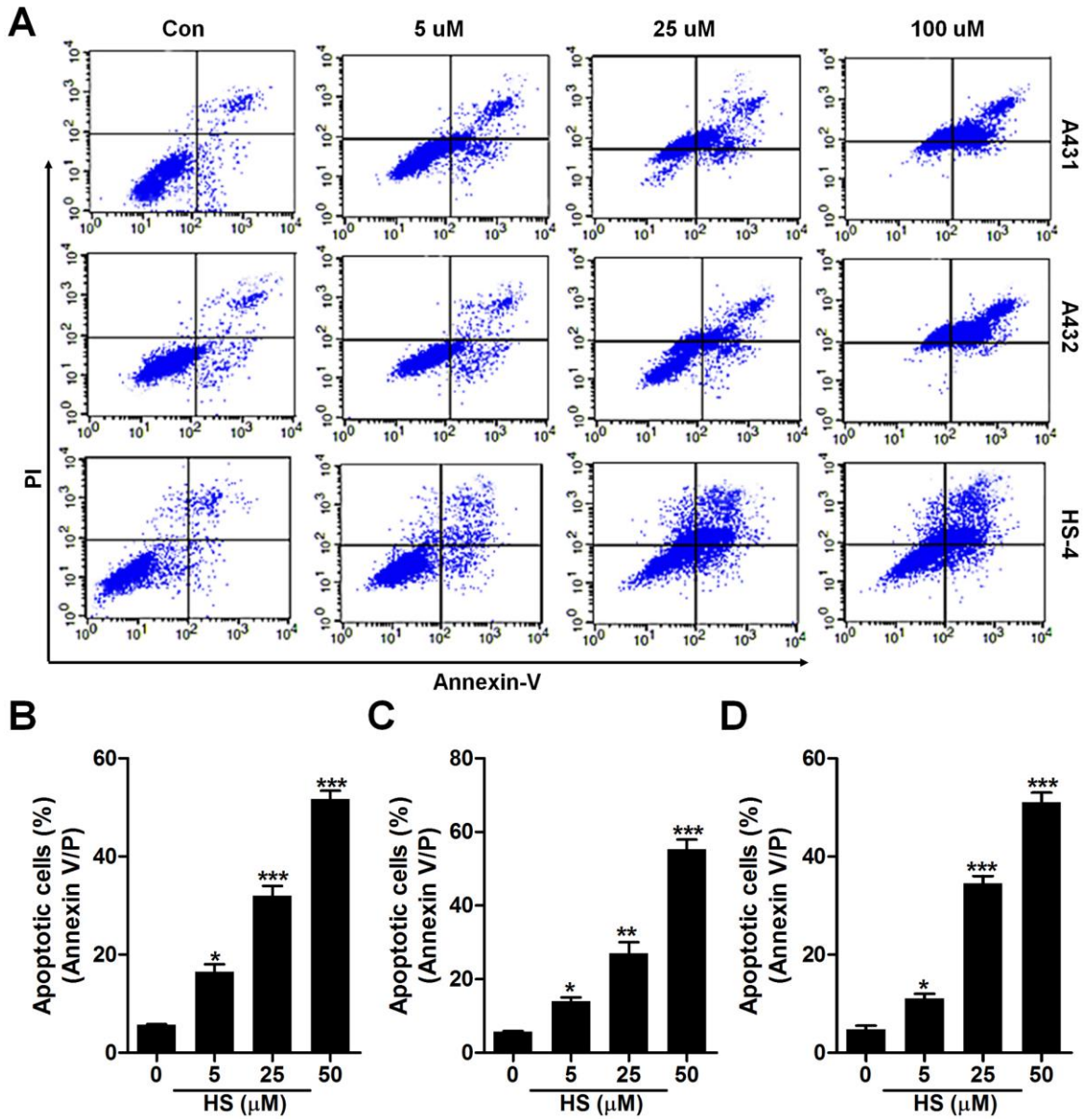

Figure 4. Hyperoside induces apoptosis in human skin cancer cells. Human skin cancer cell lines A431, A432 and HS-4 were treated with hyperoside at the indicated doses for 24 h. Then, (A) the cells were collected for flow cytometric analysis. The quantification of (B) A431, (C) A432 and (D) HS-4 was exerted following the flow cytometry. Results are shown as mean ± SEM (n = 8 in each group). $^{*}p < 0.05$, $^{**}p < 0.01$ and $^{***}p < 0.001$ versus the control group without any treatment.

4.2. Hyperoside reduces DMBA/TPA induced skin cancer *in vivo*

Fifteenth weeks after treatment with DMBA/TPA, animals developed skin tumors. The body weight of animals that harbored DMBA/TPA induced cancers and were treated without or with hyperoside did not change indicating safety of hyperoside for animal use (Figure 9). Treatment with DMBA/TPA increased the epidermal thickness, while this effect was suppressed by hyperoside (Figure 10 A-B). Consistent with such a hyperproliferative state in skin, there was an increase in the phosphorylated AURKA as well as

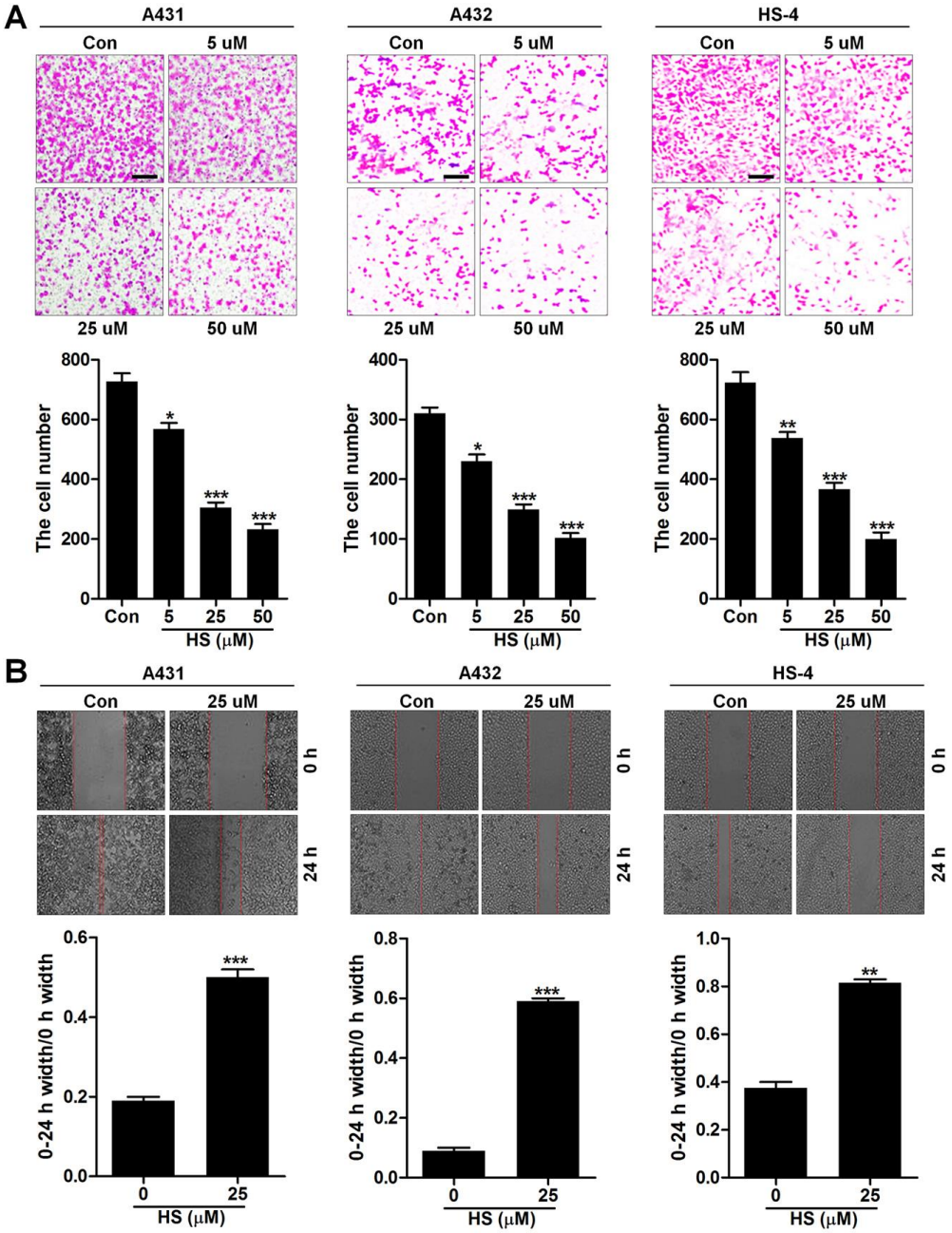

Figure 5. Hyperoside suppresses growth of skin cancer cells. Human skin cancer cell lines of A431, A432 and HS-4 were treated with hyperoside at the indicated doses for 24 h, followed by further analysis. (A) Migration of human skin cancer cell lines, A431, A432 and HS-4. (B) The analysis of scratch wound width of A431, A432 and HS-4 after hyperoside administration. Results are shown as mean ± SEM (n = 8 in each group). $^{*}p < 0.05$, $^{**}p < 0.01$ and $^{***}p < 0.001$ versus the control group without any treatment.

the number of Ki-67 positive cells in DMBA/TPA-treated mice was higher as compared to the control group whereas treatment with hyperoside reduced such an increase (Figure 10 C).

The size of the tumors was significantly reduced with 8 μM or 16 μM hypreoside in the DMBA/TPA treated mice indicating that hyperoside suppresses tumorigenesis (Figure 11). The tumors

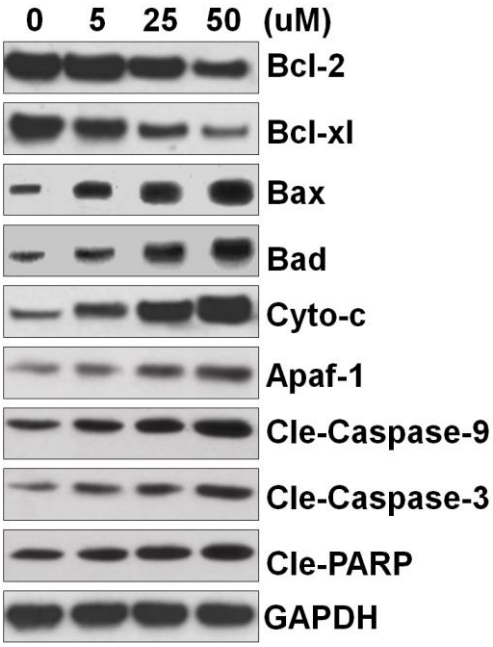

Figure 6. Hyperoside alters apoptosis-related regulators. Human skin cancer cells, A431, were treated with hyperoside at the described doses for 24 h followed by, Western blot analysis for Bcl-2, Bcl-xl, Bax, Bad, Cyto-c, Apaf-1, Caspase-9, Caspase-3 and PARP cleavage. Results are shown as mean ± SEM (n = 8 in each group). $^{*}p < 0.05$, $^{**}p < 0.01$ and $^{***}p < 0.001$ versus the control group without any treatment.

showed increased apoptosis, down-regulation of Bcl-2 and Bcl-xl and up-ergulation of Bax, Bad, Cyto-c and Apaf-1, activation of caspase-9, caspase-3 and PARP cleavage and these effects were reduced by treatment with hyperoside (Figure 12 A). Hyperoside treatment also increased autophagy-associated proteins including PTEN, Beclin-1 and LC3II (Figure 12 B). Furthermore hypreoside reversed the DMBA/TPA-induced changes in phosphorylated levels of PI3K, AKT, mTOR and AMPK while reducing p38 phosphorylation (Figure 12 C-D).

5. DISCUSSION

Skin cancer is caused by a variety of carcinogens including chemicals, radiation, and UV light. Given that the incidence of skin cancer has been rising, there is a need for evaluating strategies that can offer a safe chemopreventive effect. Here, we tested Quercetin-3-O-β-D-galactopyranoside, as a candidate with such an effect. *In vitro* treatment of cancer cells with hyperoside inhibited proliferation, and induced apoptosis and reduced autophagy. *In vivo*, hyperoside markedly inhibited diffuse epidermal hyperplasia that is often seen in skin cancers as well as of tumor burden *in vivo* in DMBA/TPA induced skin tumors. Consistent with such an impact on proliferation, phosphorylated AURKA that is increased in cells undergoing mitosis, was reduced in skin cancer cells treated with hyperoside (18). These findings show that hyperoside stops cancer progression through various mechanisms, including regulation of proliferation, and by inducing apoptosis and autophagy. The effect of hyperoside is likely mediated by increasing Bcl-2 and Bcl-xl that protect cells from apoptosis as well as by reducing the pro-apoptotic signals, Bax and Bad. Hyperoside also significantly halted activation of apoptotic cascade induced by executors of apoptosis including cytochrome C, caspase-9, caspase-3 and markedly reduced PARP cleavage which occurs in cells that undergo apoptosis. These data suggest that hyperoside might be of therapeutic value in chemoprevention of skin cancer.

The mammalian target of rapamycin (mTOR) is considered as a pro-survival signal transduction pathway that prevents apoptosis (19). Following stress, mTOR depletion inhibits cell growth and proliferation and increases autophagy and apoptosis (20). The PI3K/AKT are also involved in regulation of cell cycle, protein synthesis, apoptosis and proliferation (19, 21-22). We show here, that hyperoside normalizes phosphorylated levels of PI3K/AKT/mTOR (23-24, 25) and effectively reduces p38 phosphorylation, a MAPK known to play a crucial role in several cellular processes, including cell proliferation (26-27).

AMPK was highly phosphorylated, while p38 was de-phosphorylated by hyperoside administration, further confirming the suppressive effects of hyperoside on skin cancer, which was directly proved by reduced tumor incidence and the number of tumor lesions formed in DMBA/TPA treated mice, *in vivo*. Additionally, hyperoside induced reduction in epidermal thickness and the number of Ki-67 positive cells further showing that it has the ability to restrain tumor cell growth or skin hyperplasia.

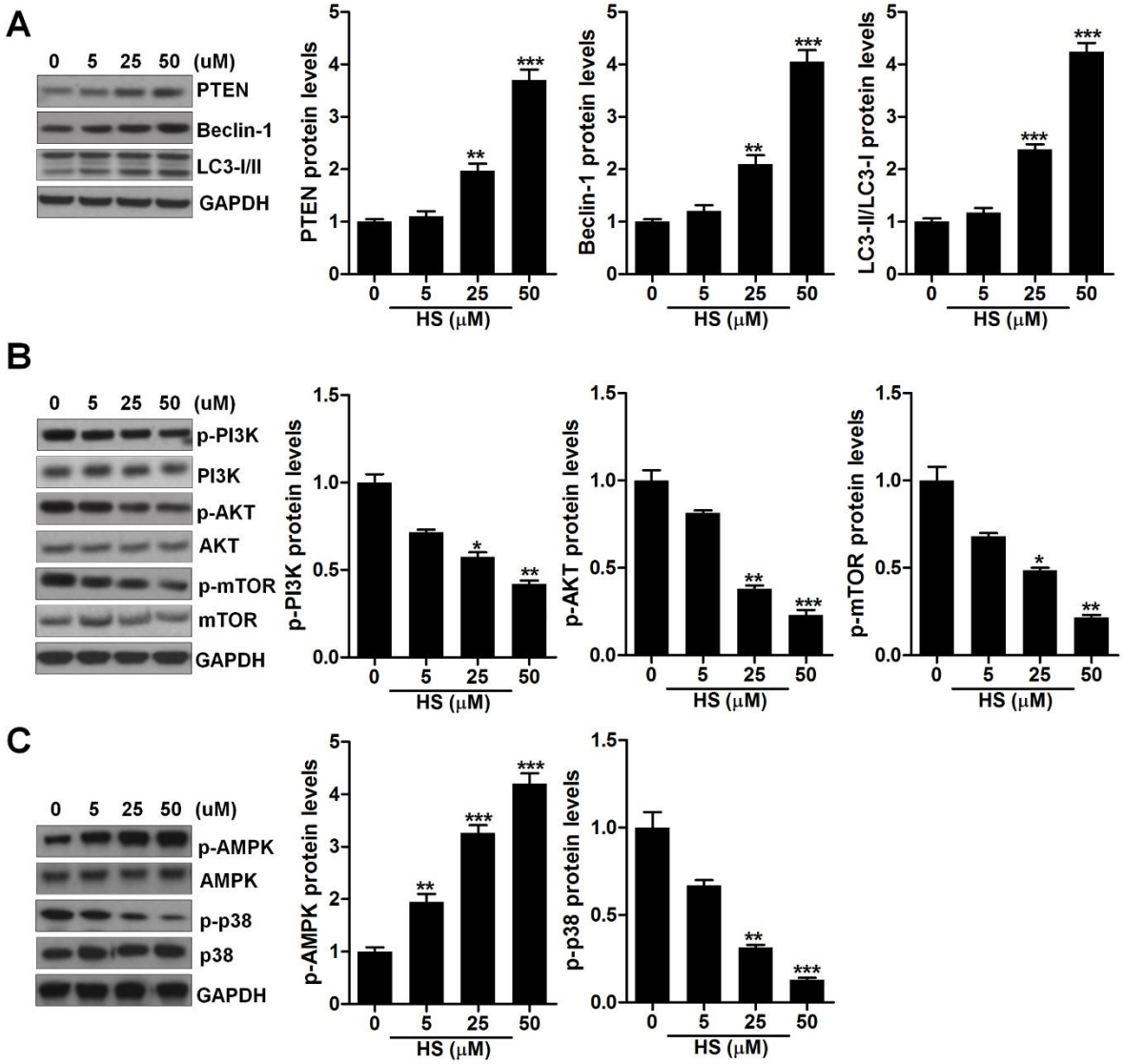

Figure 7. Hyperoside modulates autophagy, PI3K/Akt/mTOR Axis, AMPK and p38 signaling in skin cancer cells. Human skin cancer cells, A431, were treated with hyperoside at the described doses for 24 h followed by Western blot analysis for (A) PTEN, Beclin-1, LC3-I/II, and (B) PI3K, AKT and mTOR phosphorylation, (C) AMPK and level of phosphorylation of p38. Results are shown as mean ± SEM (n = 8 in each group). $^{*}p < 0.05$, $^{**}p < 0.01$ and $^{***}p < 0.001$ versus the control group without any treatment.

The treatment of cancer cells with hyperoside also increased phosphorylated AMPK, an evolutionarily conserved serine/threonine protein kinase, that serves as an energy sensor in all eukaryotic cells, maintains energy homeostasis and regulates both proliferation and apoptosis (28). Thus, treatment with hyperoside might confer resistance to the tumor development and halts further progression of tumors.

Hyperoside also alters autophagy, a conserved cellular process involved in cell survival and death whereby cellular organelles and proteins are engulfed by autophagosomes, digested within lysosomes, and recycled to sustain cellular

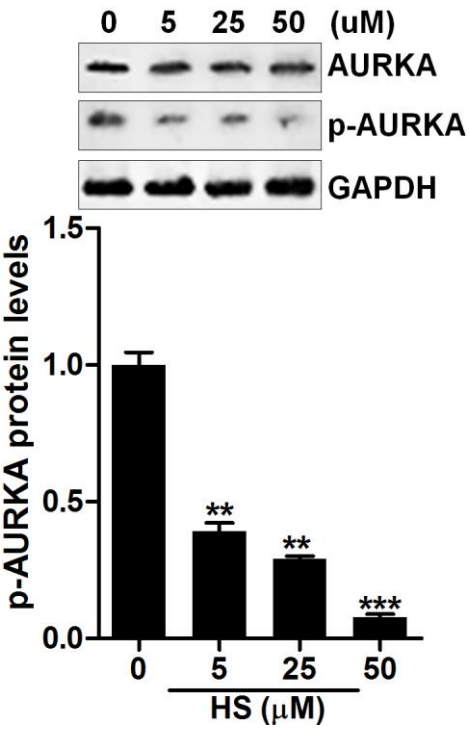

Figure 8. Hyperoside suppresses phosphorylated AURKA and alters apoptosis-related regulators. Human skin cancer cells, A431, were treated with hyperoside at the described doses for 24 h followed by Western blot analysis for determining the phosphorylation of AURKA. Results are shown as mean ± SEM (n = 8 in each group). $^{*}p < 0.05$, $^{**}p < 0.01$ and $^{***}p < 0.001$ versus the control group without any treatment.

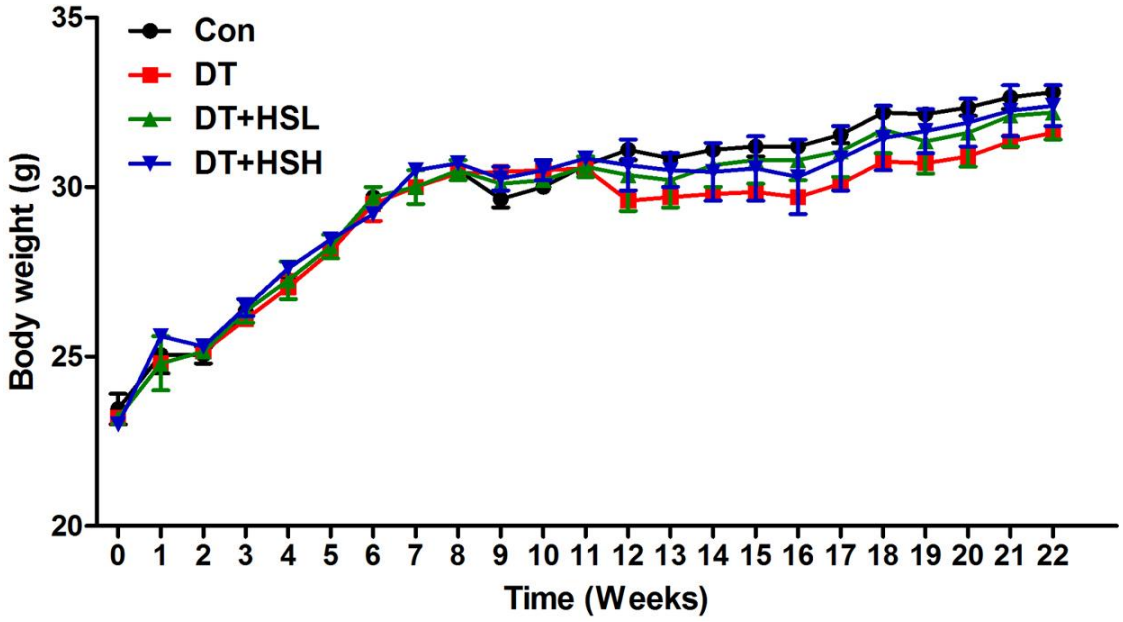

Figure 9. Hyperoside reduces skin cancer growth in DMBA/TPA-treated mice. Body weights shown as mean ± SEM (n = 20 in each group). $^{*}p < 0.05$, $^{**}p < 0.01$ and $^{***}p < 0.001$ versus the control group without any treatment.

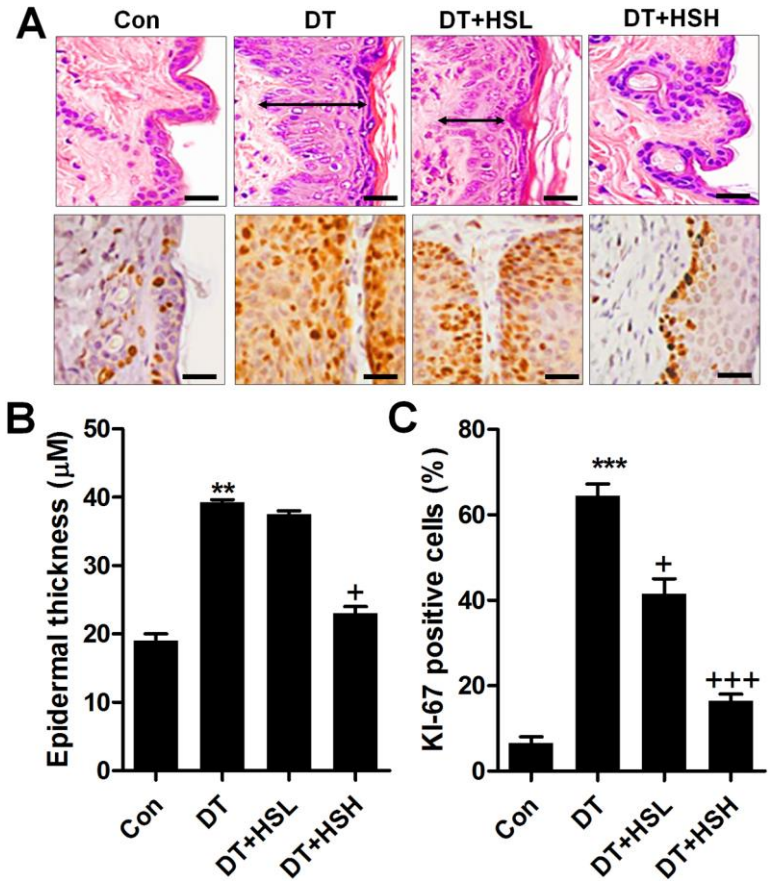

Figure 10. Hyperoside inhibits growth of DMBA/TPA-induced skin cancer. (A) Top: Representative images of epidermal proliferation. Bottom: immunostaining of Ki-67. (B) The epidermal thickness was quanifited using H&E staining. (C) Quantification of number of Ki-67 positive cells. Results are shown as mean ± SEM (n = 8 in each group). $^{*}p < 0.05$, $^{**}p < 0.01$ and $^{***}p < 0.001$ versus the control group without any treatment.

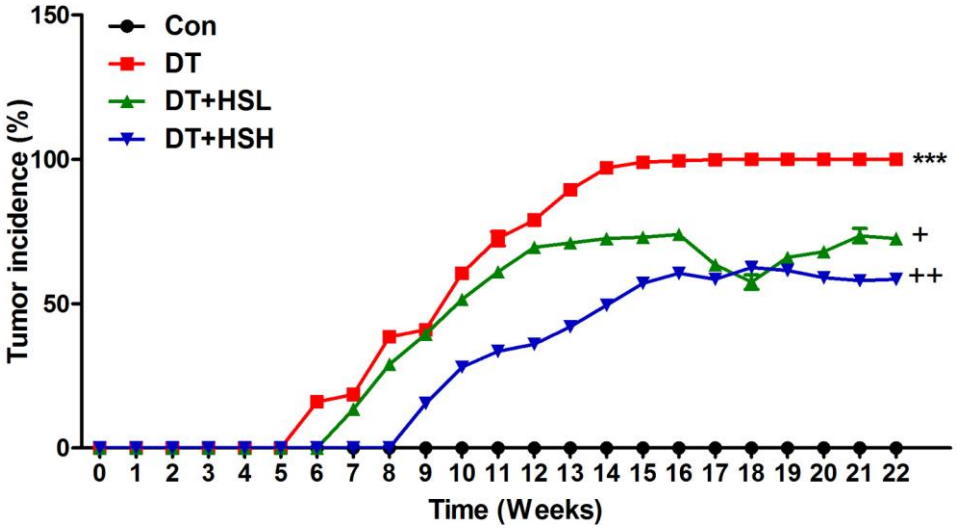

Figure 11. Effect of hyperoside on incidence of DMBA/TPA induced tumors in mice. Results are shown as mean ± SEM (n = 20 in each group). $^{*}p < 0.05$, $^{**}p < 0.01$ and $^{***}p < 0.001$ versus the control group without any treatment.

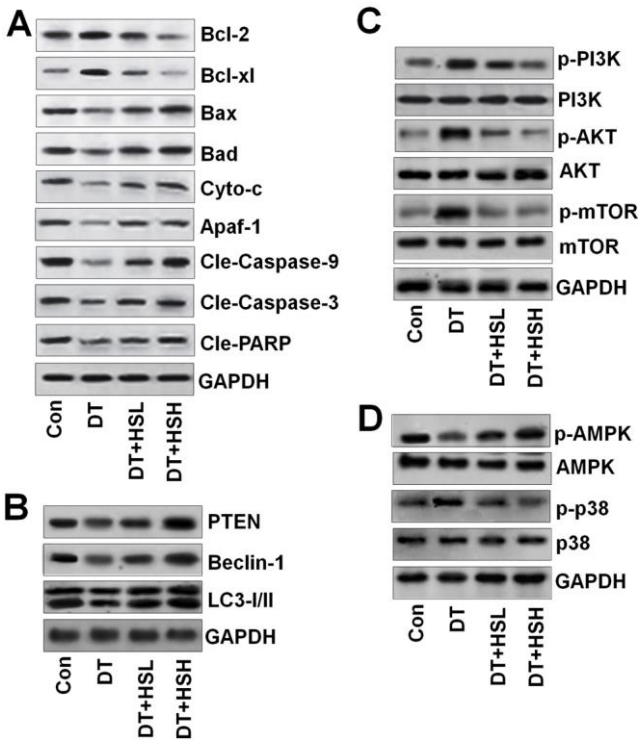

Figure 12. Effect of hyperoside in DMBA/TPA-treated mice on Western blotting of (A) Bcl-2, Bcl-xl, Bax, Bad, cleaved Cyto-c, Apaf-1, Caspase-9, Caspase-3 and PARP, (B) PTEN, Beclin-1, LC3-I/II, and (C) PI3K, AKT and phosphorylated mTOR (D) Phosphorylated AMPK and p38. Results are shown as mean ± SEM (n = 8 in each group). $^{*}p < 0.05$, $^{**}p < 0.01$ and $^{***}p < 0.001$ versus the control group without any treatment.

homeostasis (29-32). Regulators of autophagy include microtubule-associated protein II light chain 3 (LC3-II) that regulates autophagy by binding to the membranes of the autophagosomes (30, 33), Beclin 1 which acts as a tumor suppressor (34) and PTEN that, by virtue of inducing autophagy, causes inhibition of tumor growth (35). The effect of hyperoside treatment included preventing cancer induced changes of LC3I/II, Beclin-1 and PTEN.

In conclusion, this study demonstrates that hyperoside shows potential in reducing tumor burden by increasing apoptosis and autophagy and by activating the signaling required in such processes.

6. REFERENCES

1. Rogers HW, Weinstock MA, Harris AR, Hinckley MR, Feldman SR, Fleischer AB and Coldiron BM: Incidence estimate of nonmelanoma skin cancer in the United States, 2006. Arch Dermatol. 146:283-287 (2010)
DOI: 10.1001/archdermatol.2010.19

2. National Comprehensive Cancer Network Guidelines of Cancers by Site Available online. http://www.nccn.org/professionals/physicianAccessed (2014)

3. Tanvetyanon T, Padhya T, McCaffrey J, Kish JA, Deconti RC, Trotti A and Rao NG: Postoperative concurrent chemotherapy and radiotherapy for high-risk cutaneous squamous cell carcinoma of the head and neck. Head Neck, 37:840-845 (2015).
DOI: 10.1002/hed.23684
PMid:24623654

4. Jarkowski A III, Hare R, Loud P, Skitzki JJ, Kane JM III, May KS, Zeitouni NC, Nestico J, Vona KL, Groman A and Khushalani NI: Systemic therapy in advanced cutaneous squamous cell carcinoma (CSCC): The Roswell Park experience and a review of the literature. Am J Clin Oncol, 39(6), 545-548 (2016)
DOI: 10.1097/COC.0000000000000088
PMid:24879468

5. Banik BK and Becker FF: Synthesis, electrophilic substitution and structure-activity relationship studies of polycyclic aromatic compounds towards the development of anticancer agents. Curr Med Chem, 8, 1513-1533 (2001)
DOI: 10.2174/0929867013372120
PMid:11562280

6. Zhaorigetu S, Yanaka N, Sasaki M, Watanabe H and Kato N: Silk protein, sericin, suppresses DMBA-TPA-induced mouse skin tumorigenesis by reducing oxidative stress, inflammatory responses and endogenous tumor promoter TNF-α. Oncology Reports, 10, 537-543 (2003)

7. Perez-Losada J and Balmain A: Stem-cell hierarchy in skin cancer. Nat Rev Cancer, 3, 434-443(2003)
DOI: 10.1038/nrc1095
PMid:12778133

8. Budunova IV, Perez P, Vaden VR, Spiegelman VS, Slaga TJ and Jorcano JL: Increased expression of p50-NF-kappaB and constitutive activation of NF-kappaB transcription factors during mouse skin carcinogenesis. Oncogene, 18, 7423-7431 (1999)
DOI: 10.1038/sj.onc.1203104
PMid:10602501

9. Casero RA Jr and Marton LJ: Targeting polyamine metabolism and function in cancer and other hyperproliferative diseases. Nat Rev Drug Discov, 6, 373-390 (2007)
DOI: 10.1038/nrd2243
PMid:17464296

10. Livraghi T, Makisalo H and Line PD: Treatment options in hepatocellular carcinoma today. Scand J Surg, 100, 22-29 (2011)
DOI: 10.1177/145749691110000105
PMid:21482502

11. Wang ZD, Huang C, Li ZF, Yang J, Li BH, Liang RR, Dai ZJ, Liu ZW: Chrysanthemum indicum ethanolic extract inhibits invasion of hepatocellular carcinoma via regulation of MMP/TIMP balance as therapeutic target. Oncol Rep, 23, 413-421 (2010)
DOI: 10.3892/or_00000650

12. Li W, Liu M, Xu YF, Feng Y, Che JP, Wang GC, Zheng JH: Combination of quercetin and hyperoside has anticancer effects on renal cancer cells through inhibition of oncogenic microRNA-27a. Oncol Rep, 31, 117-124 (2014)
DOI: 10.3892/or.2013.2811
PMid:24173369

13. Li ZL, Hu J, Li YL, Xue F, Zhang L, Xie JQ, Liu ZH, Li H, Yi DH, Liu JC, Wang SW: The effect of hyperoside on the functional recovery of the ischemic/reperfused isolated rat heart: potential involvement of the extracellular signal-regulated kinase 1/2 signaling pathway. Free Radic Biol Med, 57, 132-140 (2013)
DOI: 10.1016/j.freeradbiomed.2012.12.023
PMid:23291593

14. Liu Y, Liu GH, Mei JJ, Wang J: The preventive effects of hyperoside on lung cancer *in vitro* by inducing apoptosis and

inhibiting proliferation through Caspase-3 and P53 signaling pathway. Biomedicine & Pharmacotherapy, 83, 381-391 (2016)
DOI: 10.1016/j.biopha.2016.06.035
PMid:27419887

15. Sharifi S, Barar J, Hejazi MS and Samadi N: Roles of the Bcl-2/Bax ratio, caspase-8 and 9 in resistance of breast cancer cells to paclitaxel. Asian Pac J Cancer Prev, 15, 8617-8622 (2014)
DOI: 10.7314/APJCP.2014.15.20.8617
PMid:25374178

16. Robles-Escajeda E, Lerma D, Nyakeriga AM, Ross JA, Kirken RA, Aguilera RJ, Varela-Ramirez A: Searching in mother nature for anti-cancer activity: anti-proliferative and pro-apoptotic effect elicited by green barley on leukemia/lymphoma cells. PLoS One, 8, e73508 (2013)
DOI: 10.1371/journal.pone.0073508
PMid:24039967 PMCid:PMC3767772

17. Tanida I, Ueno T and Kominami E: LC3 conjugation system in mammalian autophagy. Int J Biochem Cell Biol 36, 2503-2518 (2004)
DOI: 10.1016/j.biocel.2004.05.009
PMid:15325588

18. Liang CZ, Zhang X, Li H, Tao YQ, Tao LJ, Yang ZR, Zhou XP, Shi ZL, Tao HM: Gallic acid induces the apoptosis of human osteosarcoma cells *in vitro* and *in vivo* via the regulation of mitogen-activated protein kinase pathways. Cancer Biother Radiopharm, 27, 701-710 (2012)
DOI: 10.1089/cbr.2012.1245
PMid:22849560 PMCid:PMC3516425

19. Jacinto E, Loewith R, Schmidt A, Lin S, Rüegg MA, Hall A, Hall MN: Mammalian TOR complex 2 controls the actin cytoskeleton and is rapamycin insensitive. Nat Cell Biol, 6, 1122-1128 (2004)
DOI: 10.1038/ncb1183
PMid:15467718

20. Morgensztern D and McLeod HL: PI3K/Akt/mTOR pathway as a target for cancer therapy. Anticancer Drugs 16, 797-803 (2005)
DOI: 10.1097/01.cad.0000173476.67239.3b
PMid:16096426

21. CV SB, Babar SM, Song EJ, Oh E and Yoo YS: Kinetic analysis of the MAPK and PI3K/Akt signaling pathways. Mol Cells, 25, 397-406 (2008)

22. Lee ER, Kim JY, Kang YJ, Ahn JY, Kim JH, Kim BW, Choi HY, Jeong MY and Cho SG: Interplay between PI3K/Akt and MAPK signaling pathways in DNA-damaging drug-induced apoptosis. Biochim Biophys Acta, 1763, :958-968 (2006)
DOI: 10.1016/j.bbamcr.2006.06.006
PMid:16905201

23. Yue Z, Jin S, Yang C, Levine AJ and Heintz N: Beclin 1, an autophagy gene essential for early embryonic development, is a haploinsufficient tumor suppressor. Proc Natl Acad Sci USA, 100, 15077-15082 (2003)
DOI: 10.1073/pnas.2436255100
PMid:14657337 PMCid:PMC299911

24. Klionsky DJ, Abeliovich H, Agostinis P, et al: Guidelines for the use and interpretation of assays for monitoring autophagy in higher eukaryotes. Autophagy, 4, 151-175 (2008)
DOI: 10.4161/auto.5338
PMid:18188003

25. Yang F, Guo X, Yang G, Rosen DG and

Liu J: AURKA and BRCA2 expression highly correlate with prognosis of endometrioid ovarian carcinoma. Mod Pathol, 24, 836-845 (2011)
DOI: 10.1038/modpathol.2011.44
PMid:21441901 PMCid:PMC3152794

26. Cuadrado A and Nebreda AR: Mechanisms and functions of p38 MAPK signalling. Biochem J, 429, 403-417 (2010)
DOI: 10.1042/BJ20100323
PMid:20626350

27. Sui XB, Kong N, Ye L, Han W, Zhou J, Zhang Q, He C, Pan H: p38 and JNK MAPK pathways control the balance of apoptosis and autophagy in response to chemotherapeutic agents. Cancer Lett, 344174-179 (2014)
DOI: 10.1016/j.canlet.2013.11.019
PMid:24333738

28. Hardie DG: The AMP-activated protein kinase pathway - new players upstream and downstream. J Cell Sci, 117, 5479-5487 (2004)
DOI: 10.1242/jcs.01540
PMid:15509864

29. Huang X, Bai HM, Chen L, Li B and Lu YC: Reduced expression of LC3B-II and Beclin 1 in glioblastoma multiforme indicates a down-regulated autophagic capacity that relates to the progression of astrocytic tumors. J Clin Neurosci, 17, 1515-1519, (2010)
DOI: 10.1016/j.jocn.2010.03.051
PMid:20863706

30. Xu MX, Zhu YF, Chang HF, Liang Y: Nanoceria restrains PM2. 5-induced metabolic disorder and hypothalamus inflammation by inhibition of astrocytes activation related NF-κB pathway in Nrf2 deficient mice. Free Radical Biology and Medicine, 99, 259-272, (2016)
DOI: 10.1016/j.freeradbiomed.2016.08.021
PMid:27554971

31. Katayama H, Sasai K, Kawai H, Yuan ZM, Bondaruk J, Suzuki F, Fujii S, Arlinghaus RB, Czerniak BA, Sen S: Phosphorylation by aurora kinase A induces Mdm2-mediated destabilization and inhibition of p53. Nat Genet 36, 55-62 (2004)
DOI: 10.1038/ng1279
PMid:14702041

32. Gong K, Chen C, Zhan Y, Chen Y, Huang Z and Li W: Autophagy-related gene 7 (ATG7) and reactive oxygen species/extracellular signal-regulated kinase regulate tetrandrine-induced autophagy in human hepatocellular carcinoma. J Biol Chem, 287, 35576-35588 (2012)
DOI: 10.1074/jbc.M112.370585
PMid:22927446 PMCid:PMC3471698

33. Tanida I, Minematsu-Ikeguchi N, Ueno T and Kominami E: Lysosomal turnover, but not a cellular level, of endogenous LC3 is a marker for autophagy. Autophagy, 1, 84-91 (2005)
DOI: 10.4161/auto.1.2.1697
PMid:16874052

34. Furuya D, Tsuji N, Yagihashi A and Watanabe N: Beclin 1 augmented cis-diamminedichloroplatinum induced apoptosis via enhancing caspase-9 activity. Exp Cell Res 307, 26-40 (2005)
DOI: 10.1016/j.yexcr.2005.02.023
PMid:15922724

35. Zhang S and Yu D: PI(3)king apart PTEN's role in cancer. Clin Cancer Res, 16, 4325-4330 (2010)
DOI: 10.1158/1078-0432.CCR-09-2990
PMid:20622047

Abbreviations: HS, Hyperoside; PI3K, phosphoinositide 3-kinase; Akt, protein kinase B; mTOR, mammalian target of rapamycin; AMPK, 5'1 AMP-activated protein kinase; NMSC, Nonmelanoma skin cancer; SCC, squamous cell carcinoma; BCC, basal cell carcinoma; UVR, ultraviolet radiation; PAHs, polycyclic aromatic hydrocarbons; DMBA, 7, 12 dimethylbenz(a)anthracene; TPA, 12-O-tetradecanoylphorbol-13-acetate; PCD, programmed cell death; PARP, poly (ADP-ribose) polymerase; ATCC, American Type Culture Collection.

Key Words: Hyperoside, Skin Cancer, Apoptosis, Autophagy

Send correspondence to: Pengfei Wu, Department of Orthopaedics, The Affiliated Huaian No. 1 People's Hospital of Nanjing Medical University, Huai'an, Jiangsu 223300 P.R. China, Tel: 86-0517-84922766, Fax: 86-0517-84922766, E-mail: wpfdoctor@yeah.net